Babeş-Bolyai University Cluj-Napoca
Biomolecular Physics Department - BPD

Applications of IR and Raman methods from molecules to microorganisms

Revision

- Vibrational Spectroscopy – generalities
- IR Methods
  - FTIR, NIR
  - ATR-IR/AFM
- Raman methods
  - Raman, FT-Raman, Resonance Raman, SERS, Raman-AFM
- Non-linear Raman methods
  - CARS
  - Hyper-Raman
- Raman and FTIR biomedical applications

Raman/FTIR on hair

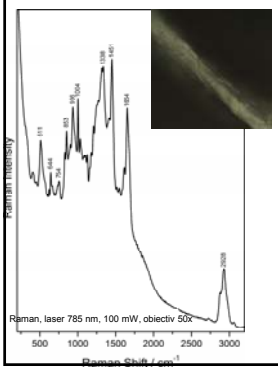

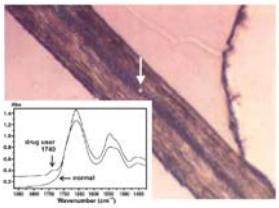

Photomicrograph of longitudinal section of human hair representing 1 day's growth. IR spectrum is from a 5.5 um spot representing 22.5 min in the life of drug user.

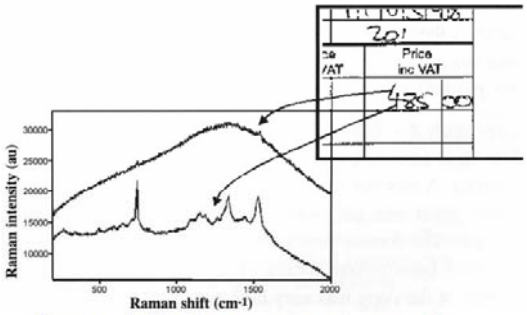

Raman spectra taken from a suspect on an insurance claim document

M. Claybourn, M. Ansell, *Science & Justice*, 2000, 40, 261-271

Forensic applications

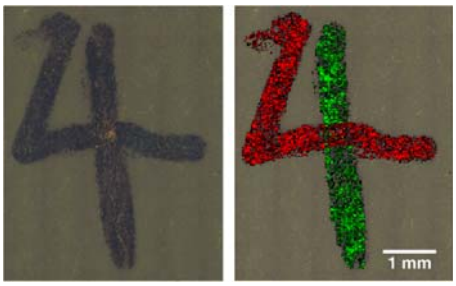

White light and Raman image of crossing inks. The Raman image shows that two different inks were used to form the figure and reveals their deposition order.

Forensic applications

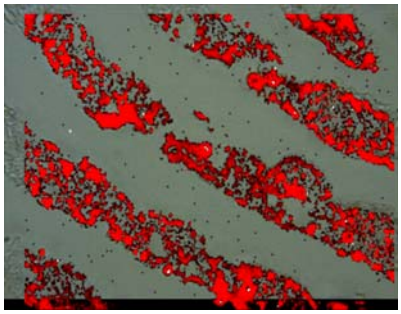

Trace amount of cocaine particles in a fingerprint. Fingerprint residue (red) and cocaine particles (white) were collected at high spatial resolution.

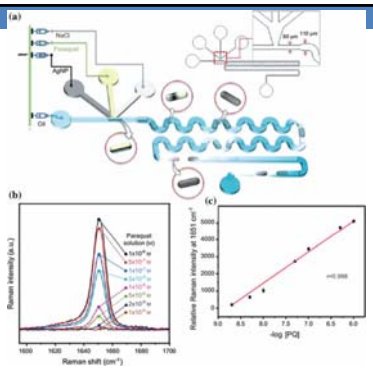

Microfluidic (lab-on-a-chip) device for SERS detection.
a Schematic illustration of a microdroplet channel for SERS detection.
b SERS spectra of paraquat at different concentrations.
c Plot of SERS intensity at 1651 cm^{-1} versus the paraquat concentration.

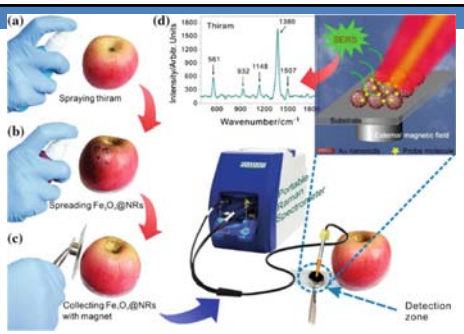

In situ SERS detection of pesticide thiram using (Fe3O4@NRs).
a Thiram solution was sprayed on apple peel.
b Fe3O4@NR suspension was spread on apple peel.
c Fe3O4@NR microspheres were transferred from contaminated apple peel to glass slide with the aid of the external magnetic field.
d The spectrum of thiram was collected by portable Raman spectrometer

Cell imaging by FTIR

Infrared spectra are obtained from individual living cells.

- Lipids (cell walls)
- Nucleic acids (DNA, RNA)
- Proteins
- Each of these major classes of cellular components have distinct IR markers

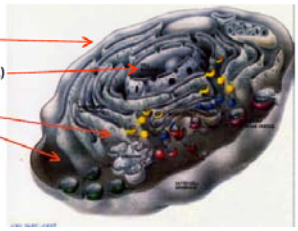

IR bands of DNA

(A) Vibration bands in the IR spectrum of mouse kidney DNA with assignment to relevant substructures.

(B) IR spectra for pancreatic DNA extracted from cancer and normal tissue, respectively. The lowest trace is the spectrum of acetate contaminated DNA from healthy tissue, resulting from the preparation.

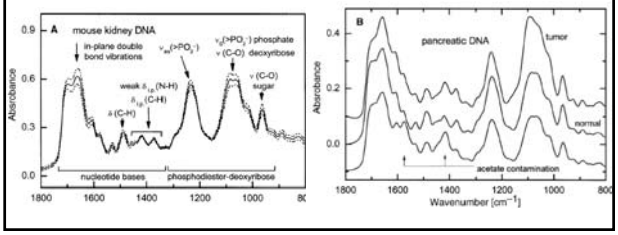

Investigating Individual Living Cells

Hoi-Ying N. Holman, *Center for Environmental Biotechnology*
Eleanor A. Blakely, Kathy Bjornstad *Life Sciences Division*
Regine Goth-Goldstein, Marion L. Russell *Environmental Energy Tech. Division*
Michael C. Martin, Wayne R. McKinney, *Advanced Light Source Division*

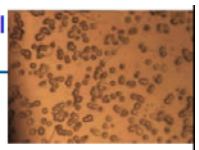

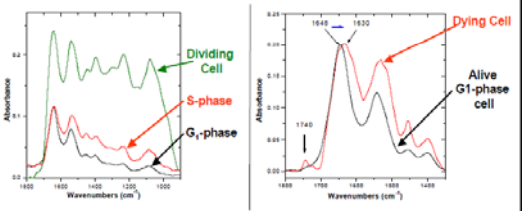

Lung Fibroblast cells (IMR-90)

ALS Beamline 1.4.3

Cellular Responses to 2,3,7,8-tetrachlorodibenzo-p-dioxin (TCDD)

Trypsinized HepG2 cells on gold (37ºC)

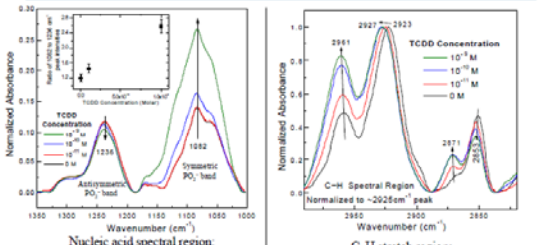

Hoi-Ying N. Holman, *Center for Environmental Biotechnology*, Eleanor A. Blakely, Kathy Bjornstad *Life Sciences Division*
Regine Goth-Goldstein, Marion L. Russell *Environmental Energy Tech. Division*
Michael C. Martin, Wayne R. McKinney, *Advanced Light Source Division*

ALS Beamline 1.4.3

Cellular imaging using Raman spectroscopy

Figure 2. Unprocessed Raman spectrum of live MCF-7 breast cancer cells. 300 second acquisition time, 785 nm illumination, approximately 100 mW illumination power.

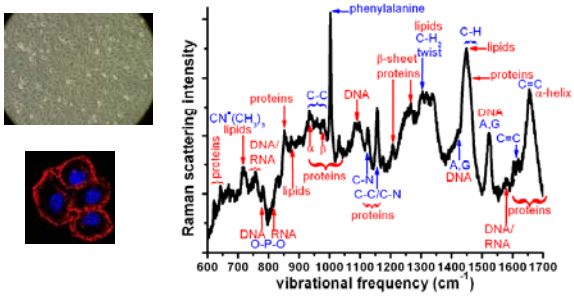

Cellular imaging using Raman spectroscopy

Figure 3. Photomicrograph of formalin-fixed lung fibroblast cell in buffer (left), Raman image after segmentation by cluster analysis (middle), Raman spectra (right) representing the nucleus (trace 1: red cluster), the cytoplasm (trace 2: cyan cluster) and lipid vesicles (trace 3: green cluster). © The Royal Society of Chemistry.

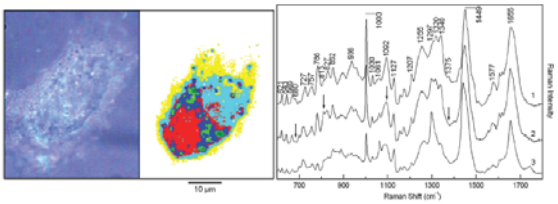

Raman imaging of a single cell of MCF7

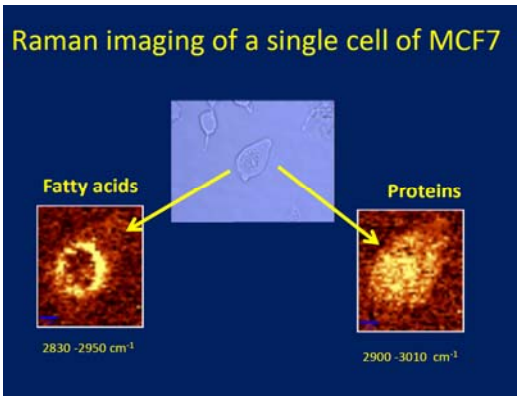

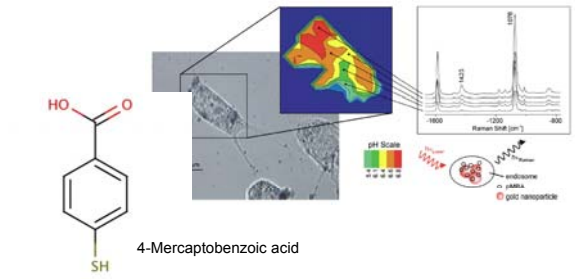

4-Mercaptobenzoic acid

Kneipp, J., Kneipp, H., Wittig, B. & Kneipp, K. Novel optical nanosensors for probing and imaging live cells. *Nanomedicine* **6,** 214–26 (2010).

Basal cell carcinoma (BCC)

Confocal Raman profiles of skin tissue with an interval of 30–40 μm. © Spr

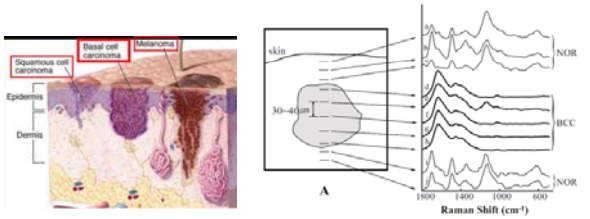

Cancer cell targeting and SERS readout

Figure 10. Cancer cell targeting and spectroscopic detection by using antibody-conjugated SERS nanoparticles. Preparation of targeted SERS nanoparticles by using a mixture of SH-PEG (thinly—polyethylene glycol) and a hetero-functional PEG (SH-PEG-COOH). Covalent conjugation of an EGFR-antibody (epidermal growth factor receptor) fragment occurs at the exposed terminal of the hetero-functional PEG. © 2010 Nature Publishing Group.

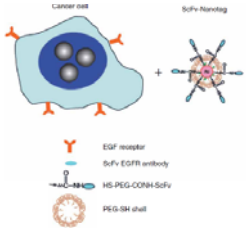

Anal. Chem. 2010, 82, 9058–9065

Hand-held Spectroscopic Device for In Vivo and Intraoperative Tumor Detection: Contrast Enhancement, Detection Sensitivity, and Tissue Penetration

Aaron M. Mohs,† Michael C. Mancini,† Sunil Singhal,‡ James M. Provenzale,§,∥ Brian Leyland-Jones,⊥ May D. Wang,# and Shuming Nie*,†

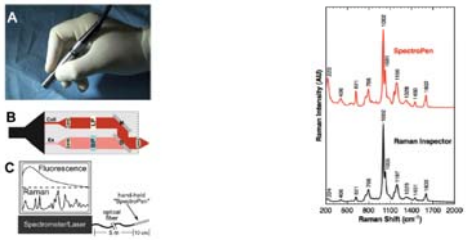

Advances in the clinical application of Raman spectroscopy for cancer diagnostics

Charlotte Kallaway, L. Max Almond, Hugh Barr, James Wood, Joanne Hutchings, Catherine Kendall*, Nick Stone

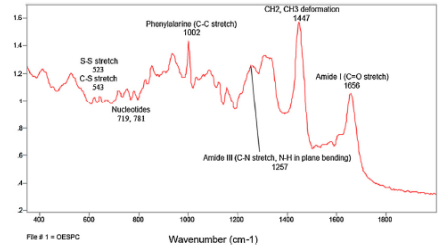

Raman spectrum of esophageal tissue measured using 830 nm excitation. Characteristic biochemical peaks have been labelled. Variations in peak height and position can be detected in tissue spectra and have been shown to indicate biochemical progression towards malignancy

Anal. Chem. 2006, 78, 7761–7769

Discrimination between Nontumor Bladder Tissue and Tumor by Raman Spectroscopy

Bas W. D. de Jong,*,† Tom C. Bakker Schut,‡ Kees Maquelin,‡ Theo van der Kwast,§ Chris H. Bangma,§ Dirk-Jan Kok,† and Gerwin J. Puppels‡

Department of Pediatric Urology, Center for Optical Diagnostics & Therapy, Department of General Surgery, Department of Pathology, and Department of Urology, Erasmus MC, Dr. Molewaterplein 50, 3015 GE, Rotterdam, The Netherlands

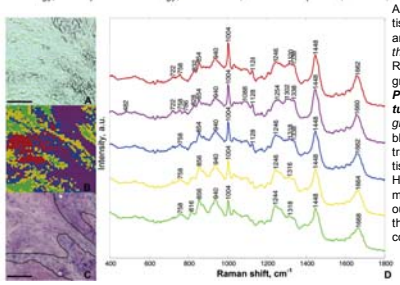

A) Unstained section of bladder tissue containing both nontumor and tumor areas, 20 *um in thickness. Scale bar, 100 um. (B)* Raman spectroscopic map; each grid element is 6.5 *um by 6.5 um.* ***Purple area is representative for tumor,*** *red area for muscle tissue, green* area for collagen fibers. and blue and yellow are areas of transition between two types of tissue. (C) Same section as (A) but HE stained after the measurements. Tissue areas are outlined. (D) Averaged spectra of the clusters in (B) with matching colors; au, arbitrary units.

Thalassemias comprise a group of genetic disorders of hemoglobin synthesis involving mutations that reduce or abolish a- or b-globin hemoglobin chain synthesis. The hallmark of b-thalassemia is an excess of a-chains due to quantitative defects in the b-globin chain; unbound a-chains denature and precipitate, shortening the lives of red blood cells.

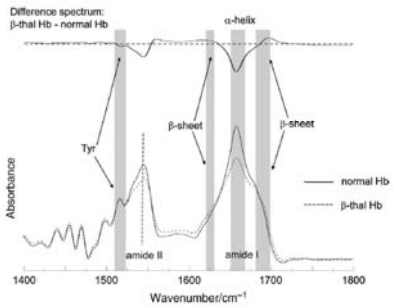

Class average mid-IR spectra for hemolyzed blood samples from b-thalassemia victims (N56) and controls (N35), as well as the difference between them. The most significant differences are amide I bands signifying **lower a-helical and higher b-sheet structure** content in b-thalassemia as compared to control hemoglobin samples.)

Diabetes is an attractive target to assess the validity and accuracy of spectroscopy-based diagnostic testing. **Serum glucose levels** are known to change with the onset of diabetes, and **serum cholester and triglycerides** can also be affected by concurrent metabolic disorders.

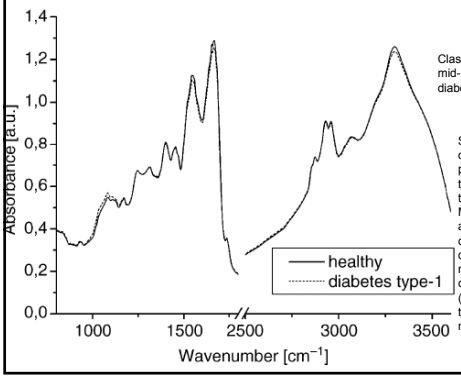

Class averages of dried serum mid-IR spectra for 40 type 1 diabetics and 42 controls

Sensitivities and specificities of 80% were achieved in the pairwise discrimination of the diabetic data sets from the set of control spectra. Most significantly, that approach proved capable of correctly categorizing the diabetic samples for which none of the three conventional serum assays (glucose, cholesterol, and triglycerides) were outside normal limits.

Class averages of dried serum mid-IR spectra for 94 **rheumatoid arthritis** patients and 94 controls, along with the difference between them.
The shaded vertical bars highlight the spectral regions that provided the basis for diagnostic classification.

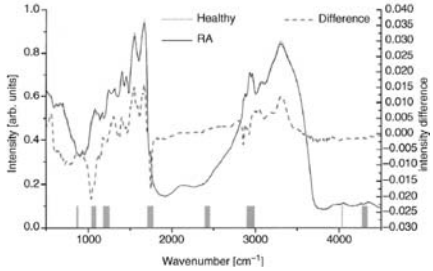

Resonance Raman spectroscopic evaluation of skin carotenoids as a biomarker of carotenoid status for human studies

Clinical use of portable RRS scanner with fiber optical module for heel skin carotenoid measurements in infants

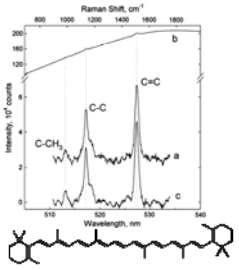

Mayne et al. Archives of Biochemistry and Biophysics, 539, 2, 163–170, 2013

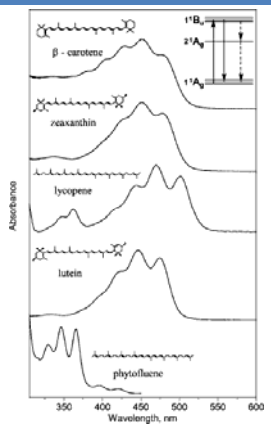

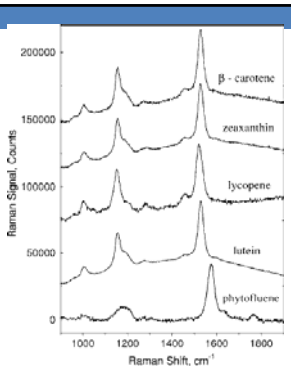

I.V. Ermakov, M. Sharifzadeh, M. Ermakova, W. Gellermann, ***Resonance Raman detection of carotenoid antioxidants in living human tissue***, Journal of Biomedical Optics, 10 (2005).

Carotenoids show a high Raman cross-section due to the resonance Raman effect

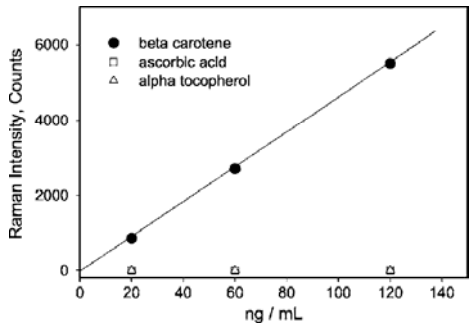

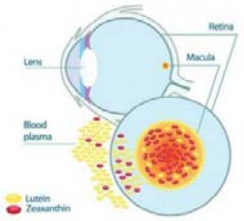

Macular pigment is comprised of Zeaxanthin and Lutein, which are found in the center of the macula (fovea) at a natural 2:1 ratio. MPOD (Macular Pigment Optical Density) is important for three specific reasons:

1. Low macular pigment is a key risk factor for Age-related Macular Degeneration (AMD), the leading cause of significant vision loss over age 55
2. Macular pigment absorbs harmful blue light, protecting the photo-receptors from damage
3. Macular pigment improves visual performance

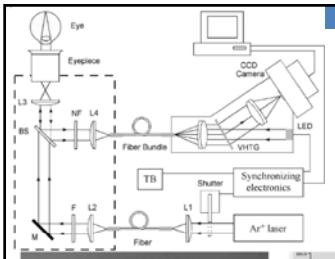

a. Schematic diagram of macular pigment resonance Raman detector designed for human clinical studies

b. Subject looking into the optical probe head of the instrument.

c Typical Raman spectra from the retina of a healthy volunteer, measured with dilated pupil 8 mm, and displayed on the computer monitor of the instrument.

spectrum obtained after a single measurement, clearly showing the carotenoid Raman signals superimposed upon a broad fluorescent background; Background corrected spectrum.

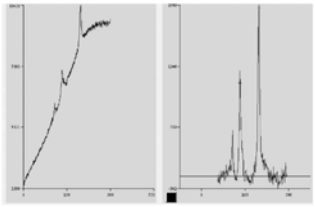

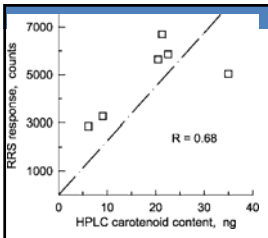

Correlation of RRS signals obtained for the C=C double bond vibration at 1525 cm^{-1} with the carotenoid content of six monkey retinae as determined by HPLC. A linear fit to the data results in a correlation coefficient of 0.68.

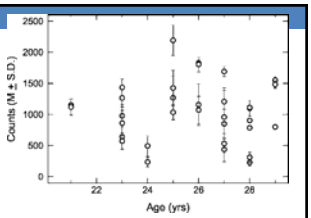

RRS MP measurements of 33 normal eyes for a young group of subjects ranging in age from 21 to 29 years. Note the large 10-fold variation of RRS levels between individuals. Since the ocular transmission properties in this age group can be assumed to very similar, the variations are can be assigned to differing MP levels. Subjects with extremely low carotenoid levels may be at higher risk of developing macular degeneration later in life.

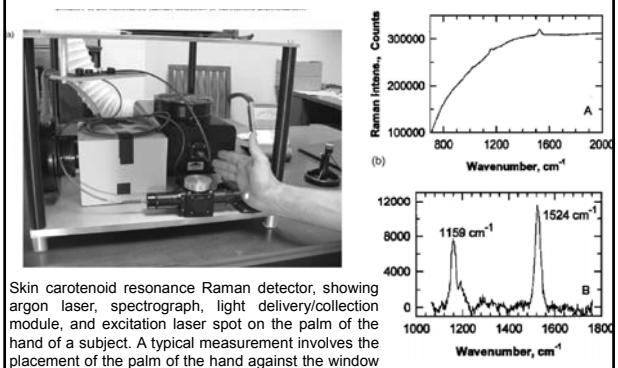

Skin carotenoid resonance Raman detector, showing argon laser, spectrograph, light delivery/collection module, and excitation laser spot on the palm of the hand of a subject. A typical measurement involves the placement of the palm of the hand against the window of the module and exposing the palm for about 1 min at laser intensities of 10 mW in a 2-mm-diam spot.

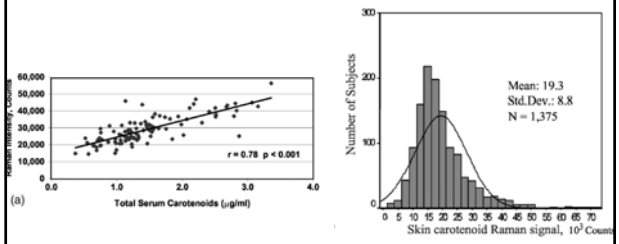

a) Correlation of skin resonance Raman intensity measured in the inner palm of the hand with serum carotenoids determined by HPLC, obtained for a group of 104 healthy male and female adults.

b) Histogram of skin carotenoid resonance Raman response measured in the palm of hands for 1375 subjects, showing **wide distribution** of skin carotenoid levels in a large population.

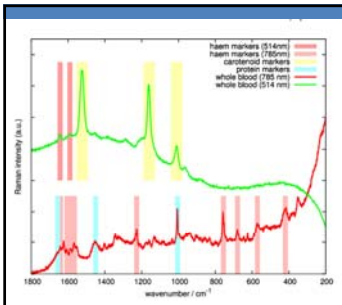

Comparison between Raman spectra arising from freshly human whole blood collected using 785 nm excitation laser line (red line) and 514 nm excitation laser line (green line). The spectra show several molecular fingerprints: the green line (514 nm) represent the -carotene molecule while in the red line (785 nm) are clearly distinguishable the presence of oxy-haem peaks.

M. Casella, A. Lucotti, M. Tommasini, M. Bedoni, E. Forvi, F. Gramatica, G. Zerbi, ***Raman and SERS recognition of β-carotene and haemoglobin fingerprints in human whole blood***, Spectrochimica Acta - Part A: Molecular and Biomolecular Spectroscopy, 79, 915 (2011).

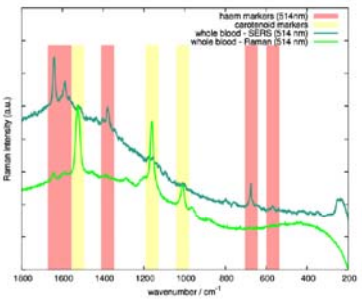

Comparison between Raman (red line) and SERS (green line) spectra arising from freshly human whole blood collected using the same laser excitation line (514 nm).
Both spectra show several fingerprints due to the different use of Raman effect. **The Raman spectrum shows the beta-carotene fingerprint, while the SERS one provides haemoglobin identification with information on the oxygenation state**.

Clinical study

Phase 1	Phase 2	Phase 3	Phase 4
Depletion Restricted food list	High carotenoid Experimental diet	Depletion Restricted food list	Repletion Return to usual diet
6 wk	8 wk	6 wk	8 wk
RRS scan (2-5x/wk)	RRS daily scan and meals	RRS scan (2-5x/wk)	RRS scan (2-5x/wk)

Week: BL 6 14 20 28

L. Jahns, L.K. Johnson, S.T. Mayne, B. Cartmel, M.J. Picklo Sr, I.V. Ermakov, W. Gellermann, L.D. Whigham, ***Skin and plasma carotenoid response to a provided intervention diet high in vegetables and fruit: Uptake and depletion kinetics***, American Journal of Clinical Nutrition, 100, 930 (2014).

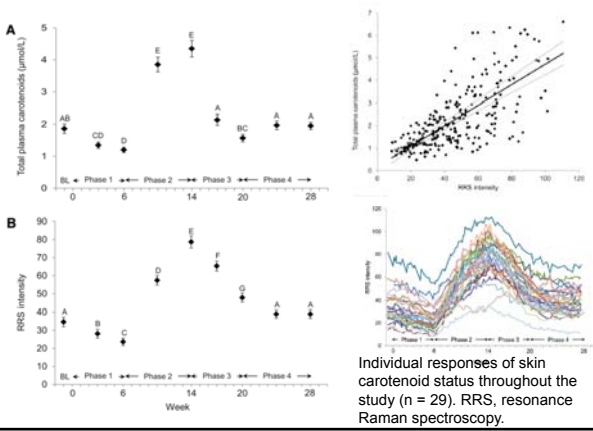

Individual responses of skin carotenoid status throughout the study (n = 29). RRS, resonance Raman spectroscopy.

https://washington-seattle.digication.com/jonliu/Home

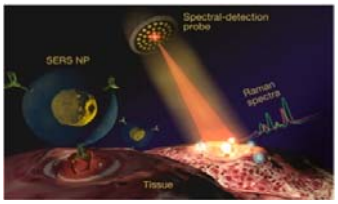

Gastrointestinal cancers, including colon and esophageal cancer, are some of the most prevalent diseases worldwide. **Early detection** is key to patient survival, and could be aided by wide-field molecular imaging technologies. However, accurate detection is hampered by the variability in molecular expression patterns exhibited between patients and within patients over time. Therefore, we are **developing *in vivo* endoscopic imaging devices** that utilize a single laser illumination source to image surface-enhanced Raman scattering (SERS) nanoparticles that are capable of being highly multiplexed to target a large number of biomarkers.

https://washington-seattle.digication.com/jonliu/Home

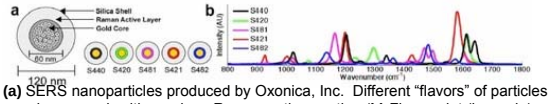

(a) SERS nanoparticles produced by Oxonica, Inc. Different "flavors" of particles are shown, each with a unique Raman-active coating (**b)** Fingerprint (barcode) Raman spectra from each of five different flavors of particles.

Spectral probe deployed through the instrument channel of an endoscope, and being used within the human colon

https://washington-seattle.digication.com/jonliu/Home

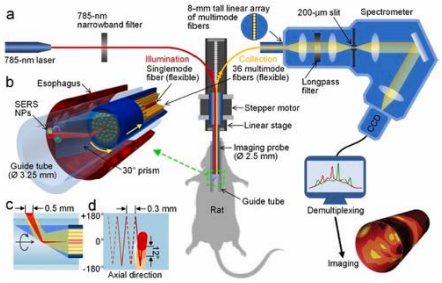

A spectral-detection system with a contact probe for quantifying the relative concentrations of multiplexed SERS NPs topicall applied on fresh intact tissues (*ex vivo* and *in vivo*). [Y Wang, et al., *Technology* 2, 1-15 (2014).]

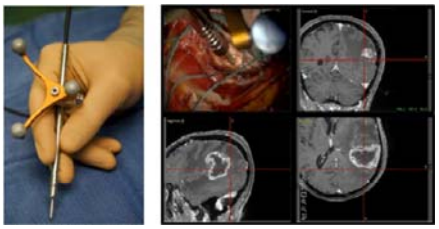

Raman spectroscopy handheld contact probe system for intraoperative detection. Picture of the probe used intraoperatively
J. Desroches, M. Jermyn, K. Mok, C. Lemieux-Leduc, J. Mercier, K. St-Arnaud, K. Urmey, M.C. Guiot, E. Marple, K. Petrecca, F. Leblond, *Characterization of a raman spectroscopy probe system for intraoperative brain tissue classification*, Biomedical Optics Express, 6 (2015).